

Photocatalytic degradation of methylene blue from aqueous solutions using nanopillars-TiO₂ thin films: Batch reactor studies

C. Lalhriatpuia

Department of Chemistry, Pachhunga University College, Aizawl 796001, Mizoram, India

Nanopillars-TiO₂ thin films was obtained on a borosilicate glass substrate with (S1) and without (S2) polyethylene glycol as template. The photocatalytic behaviour of S1 and S2 thin films was assessed in the degradation of methylene blue (MB) dye from aqueous solution under batch reactor operations. The thin films were characterized by the SEM, XRD, FTIR and AFM analytical methods. BET specific surface area and pore sizes were also obtained. The XRD data confirmed that the TiO₂ particles are in its anatase mineral phase. The SEM and AFM images indicated the catalyst is composed with nanosized pillars of TiO₂, evenly distributed on the surface of the substrate. The BET specific surface area and pore sizes of S1 and S2 catalyst were found to be 5.217 and 1.420 m²/g and 7.77 and 4.16 nm respectively. The photocatalytic degradation of MB was well studied at wide range of physico-chemical parameters. The effect of solution pH (pH 4.0 to 10.0) and MB initial concentration (1.0 to 10.0 mg/L) was extensively studied and the effect of several interfering ions, i.e., cadmium nitrate, copper sulfate, zinc chloride, sodium chloride, sodium nitrate, sodium nitrite, glycine, oxalic acid and EDTA in the photocatalytic degradation of MB was demonstrated. The maximum percent removal of MB was observed at pH 8.0 beyond which it started decreasing and a low initial concentration of the pollutant highly favoured the photocatalytic degradation using thin films and the presence of several interfering ions diminished the photocatalytic activity of thin films to some extent. The overall photocatalytic activity was in the order: S2 > S1 > UV. The photocatalytic degradation of MB was followed the pseudo-first-order rate kinetics. The mineralization of MB was studied with total organic carbon measurement using the TOC (total organic carbon) analysis.

Key words: Nanopillars-TiO₂, thin films, methylene blue, kinetics, photocatalyst.

Received 06 August 2018
Accepted 24 September 2018

*For correspondence ✉:
clhpuia@gmail.com

Contact us ✉:
sciencevision@outlook.com

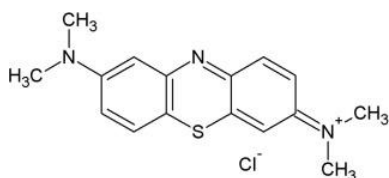
This is published under a Creative Commons Attribution-ShareAlike 4.0 International License, which permits unrestricted use and reuse, so long as the original author (s) and source are properly credited.

Introduction

The contamination of aquatic ecosystem by a variety of dyes posed a serious threat to aquatic organisms. Meanwhile, Ca 10,000 kinds of commercial dyes with over 7 x 10⁵ tons of dyes being pro-

duced annually,¹⁻⁴ and about 10-15% of the dyes are being disposed-off to the effluent from dyeing operations.⁵⁻⁷ These industrial effluent dyes are characterized by high alkalinity, biological oxidation demand, chemical oxidation demand and total dissolved solids.⁸ In addition to aesthetic deterioration

and eutrophication of water bodies some of the dyes, dye precursors, and dye degradation products are reported to be toxic and carcinogenic or mutagenic.⁹ Different methods such as sedimentation, adsorption, chemical precipitation and some biological treatment processes were employed in the remediation of such contaminated wastewaters; however, they showed some issues related to the subsequent environmental concerns or high input cost of the treatment process.¹⁰ Similarly, it was reported that the oxidation of dyes with suitable chemical oxidant *viz.* chlorine, ozone, hydrogen peroxide, electro-oxidation or wet-air oxidation were found to be inappropriate either due to the cost effectiveness or the by-products generated caused additional environmental concerns.^{11,12} Methylene blue (3,7-bis (dimethylamino) phenothiazin-5-ium chloride), a thiazine dye (structure 1) is a cationic organic dye commonly found in industrial wastewater. It is widely used as a bacteriologic stain and as an indicator.¹³ Moreover, these dyes are non-biodegradable and possess relatively high persistency or recalcitrant in soils and aquatic systems.¹⁴



Structure 1. Methylene blue.

Advanced oxidation process (AOP) based on heterogeneous catalysis employing semiconductor TiO_2 photocatalyst is found to be a green and sustainable treatment process for various wastewater treatment strategies.¹⁵ Under illumination, the photo-generated electron-hole pairs (e^-/h^+) enables the oxidation and reduction of pollutant adsorbed onto the surface of TiO_2 . The e^- and h^+ leads to the formation of radical species *viz.*, hydroxyl radical ($\bullet\text{OH}$) and peroxide radical ($\text{O}_2^{\bullet-}$). The redox potential of $\bullet\text{OH}$ radical is relatively very high ($E^\circ = 2.80 \text{ V}$) which enables efficient oxidation/degradation of even stable organic compounds/

species from aqueous solutions.¹⁶ Previously, photocatalytic degradation of methylene blue using TiO_2 powder catalyst was investigated. Results showed that maximum degradation was observed for TiO_2 powder calcined at 750°C due to presence of anatase and rutile phases in 80:20 ratio. The activity of powder calcined at 750°C was comparable with commercial Degussa P-25 TiO_2 powders.¹⁷ Similarly, photocatalytic degradation of various types of dyes (alizarin S, crocein orange G, methyl red, Congo red, methylene blue) in water by suspension of UV-irradiated TiO_2 was studied and results showed that the degradation followed pseudo-first order rate kinetics and the initial rates of disappearance was in the order $\text{CR} > \text{MB} > \text{AS} > \text{OG} > \text{MR}$.¹⁸ Continuous effort was made to overcome the recombination of electron-hole pairs with improved visible-light photocatalytic activity of F-doped TiO_2 (F- TiO_2). Results showed that the F- TiO_2 exhibits an enhanced photocatalytic performance in the degradation of MB which achieved degradation rate of 91% under visible light irradiation as compared with pure TiO_2 (32%).¹⁹

The major problem in the implications of TiO_2 nanoparticles or nanocomposites is the separation of catalyst once operation is completed and hence, the further use of catalyst is restricted in successive operations. Moreover, the reactivity of photocatalyst is greatly hindered with the shadowing effect of the semiconductor particles. This further suggested the use of a thin layer (film/sheet) of TiO_2 immobilized on a variety of supports, e.g. glass plates, aluminium sheets etc, could show potential applicability as it could be easily recovered and reused. Recently, a novel mesoporous hybrid $\text{Ag}^0(\text{NP})/\text{TiO}_2$ thin films was used in the degradation of tetracycline and sulfamethoxazole. Results showed that the template synthesized photocatalyst $\text{Ag}^0(\text{NP})/\text{TiO}_2(\text{B})$ showed significantly enhanced catalytic activity than the non-template synthesized photocatalyst $\text{Ag}^0(\text{NP})/\text{TiO}_2(\text{A})$ and the thin film $\text{Ag}^0(\text{NP})/\text{TiO}_2(\text{B})$ showed no significant decrease even after 6 cycles of successive operations.²⁰ Similarly, the degradation of methylene blue dye using nanostructured TiO_2 thin film prepared by RF mag-

neutron sputtering was studied and observed that the 40 nm thick nanostructured TiO₂ film exhibits highly enhanced photocatalytic activity taking only 45 mins to complete degradation of 2.1 μM MB in water under sun light irradiation.²¹ Therefore, the present communication was intended to immobilized thin films of TiO₂ particles onto a glass substrate using the sol-gel template method and further it was employed in the photocatalytic degradation of methylene blue (MB) dye from aqueous solutions.

Materials and Methods

Chemical and materials

The chemicals used for the experiments were of AR/GR grade. Titanium (IV) isopropoxide, Poly (ethylene glycol), methylene blue, were obtained from Sigma Aldrich. Co., USA. Acetylacetone, ethanol anhydrous, hydrochloric acid, sodium hydroxide, zinc chloride, cupric sulphate pentahydrate, cadmium nitrate tetrahydrate, ethylenediamine-tetraacetic acid, sodium nitrate, sodium nitrite, oxalic acid and glacial acetic acid were obtained from Merck India Ltd., India. Sodium chloride and glycine were obtained from Himedia, India Ltd., India.

Stock solution of MB (100.0 mg/L) was prepared in purified water. The solution was sonicated for 10 min to increase the solubility of these pollutants in water. Further, the required experimental concentration was obtained by the successive dilution of stock solution. The UV-Visible spectrophotometer (Thermo Fisher Scientific, Model: Evolution 201) was used for quantitative determination and to study the degradation kinetics of organic compounds by measuring the change in concentration at a fixed wavelength of 663 nm. The TOC analyzer (Shimadzu, Japan; model: TOC-VCPH/CPN) was fully employed to obtain the total organic carbon content data for the study of the degradation of organic compounds present in water.

Preparation of nano TiO₂ thin films

Nanopillars-TiO₂ thin films S1 (without PEG) and S2 (with PEG) were obtained on borosilicate glass disk using sol-gel dip coating method with molar ratios of these chemicals: TISP: AcAc: EtOH: AcOH: H₂O was taken as 1:1.3:40:0.9:12.5, respectively. The detailed preparation process was described previously.^{22,23}

Characterization of thin films

X-ray diffraction (XRD) data of the TiO₂ thin films was collected by X-ray diffraction machine i.e. PANalytical, Netherland (model X'Pert PRO MPD) and the diffraction data was recorded at the scan rate of 0.034 of 2θ illumination and at an applied voltage of 45 kV with a measured current 35 mA. The Cu K_α radiation was employed having wavelength of 1.5418 Å. Surface morphology of thin films was observed by scanning electron microscope (model FE-SEM SU-70, Hitachi, Japan). Atomic force microscopy (AFM) measurements were carried in the non-contact mode, using XE-100 apparatus from Park Systems (2011) having sharp tips (>8 nm tip radius; PPP-NCHR type from NanosensorsTM). The topographical 3D AFM images were taken over the area of 10×10 μm². FT-IR (Bruker, Tensor 27, USA by KBR disk method) was used to collect the IR data for these thin films. Moreover, the BET specific area was obtained using the Protech Korea BET surface area Analyzer (model ASAP 2020).

Photocatalytic degradation studies

Photocatalytic degradation of MB was carried out under batch reactor experimentation. The reactor consists of a black box (dimension: 60 x 45 x 45 cm). A 150 mL borosilicate glass beaker containing 50 mL of dye solution was placed and thin film (without PEG (S1)) or (with PEG (S2)) was placed horizontally at the bottom of the reactor. An UV-C lamp of maximum wavelength, λ = 253.7 nm (model: Phillips TUV 11W, 4 P.SE; Poland) was

placed at the top of the reactor at 10 cm above the solution. The UV-radiation reached the TiO₂ photocatalyst through the dye solution, causing the photocatalytic oxidation at the catalyst surface. The reaction temperature was maintained at 25±1°C using the self-assembled water-bath. Air was bubbled to the reactor solution using aquarium air pump. The pollutant concentration was analysed with a UV-Vis spectrophotometer at certain time interval up to 2 h. Initially, blank experiments were performed under UV irradiation (photolysis) without TiO₂ photocatalyst for comparison.

The pH of this solution was maintained by the drop wise addition of conc. HCl/NaOH solutions. The concentration dependence data was obtained varying the MB concentrations respectively from 1.0 to 10.0 mg/L. The percent efficiency of degradation of MB was calculated with the equation (1):

$$\text{Removal Efficiency} = \frac{C_i - C_f}{C_i} \times 100 \quad (1)$$

where, C_i and C_f are the concentrations of MB before and after the photocatalytic treatment.

Results and Discussion

Characterization of thin films

XRD data collected for the S1 and S2 samples were shown in the Fig. 1 or elsewhere.²³ The characteristic peaks obtained for the samples S1 and S2 at 2θ values of 25.39, 37.84, 48.14, 53.44 and 54.59 of 25.39, 37.84, 48.14, 53.44 and 54.59 were well matched with the standard ICDD (International Centre for Diffraction Data) reference pattern and are assigned to the TiO₂ anatase phase. The average particle size of the TiO₂ using Debye–Scherrer equation²² for S1 and S2 catalysts were found to be 25.4 and 21.9 nm, respectively. This further inferred that the S1 and S2 comprised with nanosized, possibly the nanopillars-TiO₂, are evenly distributed on the substrate surface.

Fig. 2 showed The SEM images of S1 and S2 and also presented previously.²³ It was observed that

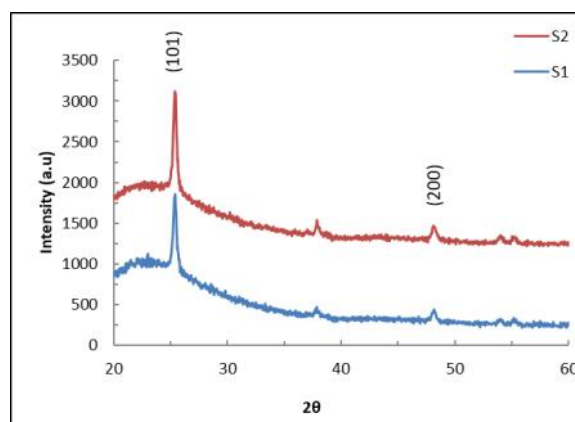


Figure 1 | X-ray diffraction pattern for the S1 and S2 thin films.²³

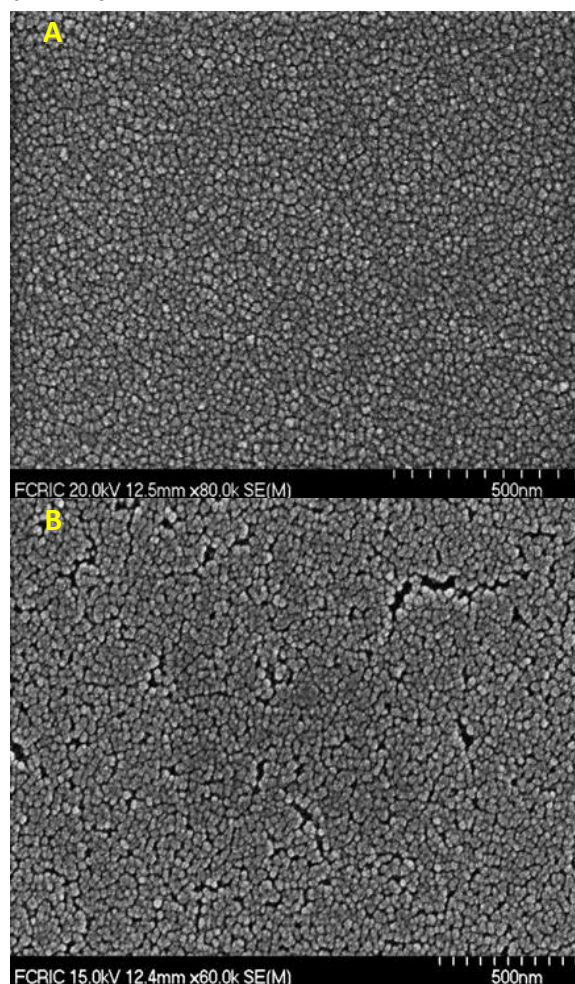


Figure 2 | FE-SEM images of the thin films (a) S1; and (b) S2.²³

the S1 catalyst contained nanosized pillars of TiO_2 which are aggregated on the solid surface. These pillars were very evenly distributed and forming a thin film onto the substrate surface with an average size of less than 15 nm. On the other hand, the S2 sample was more disordered with several cracks on the surface. The particles of TiO_2 were also, at places, aggregated.

Fig. 3 showed the 3D AFM images of S1 and S2 were shown in Fig.3 or elsewhere.²² It was obvious that S1 is composed with homogeneous distribution of nanopillars- TiO_2 with optically smooth surface. However, a non-uniform distribution of particles was seen with S2 catalyst. Further, the average height of the pillars was found to be 180 and 40 nm respectively for the S1 and S2 samples. Moreover, the calculated average roughness (Ra) and root mean square roughness (Rq) for S1 and S2 samples were found to be 3.523, 14.06 nm and

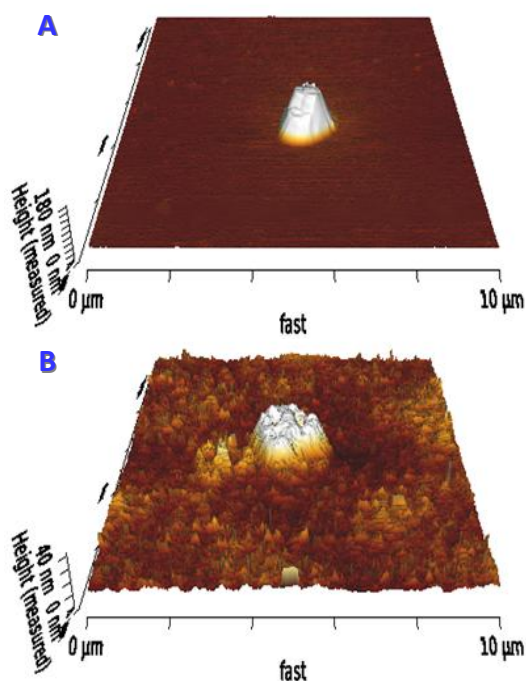


Figure 3 | 3D AFM images of S1 and S2 samples at the scale of $10 \times 10 \mu\text{m}^2$.²²

2.708, 4.668 nm, respectively.

The FT-IR data for S1 and S2 samples were presented in Fig. 4 or elsewhere.²³ The absorption spectra of S1 and S2 samples were identical with a sharp band at around 3437 cm^{-1} which was assigned to the O-H stretching vibration of Ti-OH. The bending vibration of the O-H mode was obtained at around 1638 cm^{-1} . The bands obtained at 470 and 422 cm^{-1} were assigned to bending vibrations of Ti-O and Ti-O-Ti of the titanium dioxide framework bonds or perhaps the stretching mode of Ti-O bond which was enveloped the bonds of Ti-O-Ti of the titanium dioxide network.²³ While the narrow bands at 2922 and 2862 cm^{-1} were due to organic residues.²³

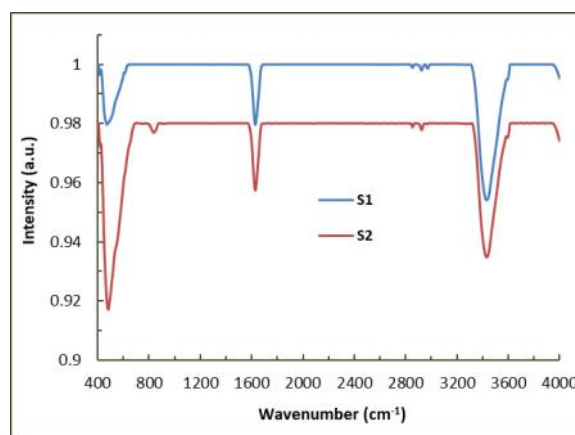


Figure 4 | FT-IR spectra of the S1 and S2 thin film samples.²³

The BET specific surface area and pore size of S1 and S2 catalyst were shown in Table 1. Since the Scherrer diameter indicated that the particle diameter is in the order of 21–29 nm. Therefore, it was assumed that a regular network is obtained on the substrate surface and, possibly, the titania is forming a nanopillars on the substrate with a maximum size of 30 nm. It was also observed that although the specific surface area of the S2 catalyst was less than S1 sample however, the meso-pore size was decreased significantly. This enhances the possibility of the pollutants to trap within the pores

and show a better catalytic activity.

Table 1 | BET specific surface area and pore size of S1 and S2 catalyst.

Sample	BET specific surface area (m ² /g)	Pore size (nm)
S1	5.217	1.420
S2	7.77	4.16

Photocatalytic degradation of MB

Effect of solution pH

The solution pH is an important factor which influenced the sorption of pollutants on the catalyst surface and hence greatly influenced the photocatalytic activity. Therefore, the effect of pH in the degradation of MB was conducted over a wide pH range, pH 4.0 to 10.0, at a constant MB initial concentration (5.0 mg/L). The pH dependence degradation of MB was presented in Fig. 5. It was observed that the percentage removal of MB increased with increased in solution pH from pH 4.0 to pH 8.0 and then it started decreasing up to pH 10.0. This inferred that an optimum pH 8.0 could be an appropriate pH for better performance of photocatalyst. The extent of degradation was affected by the surface charge properties of S1 and S2 as well as the speciation of the MB molecule at varied solution pH values. It was assumed that TiO₂ surface remained positively charged in the acidic media (pH < 6.9) and negatively charged in alkaline solutions (pH > 6.9) as the point of zero charge for S1 and S2 was obtained to 6.9.²⁴ On the other hand, the MB molecule is a cationic dye¹³ which carries net positive charge. Therefore, a higher removal of MB at alkaline pH i.e. pH 6 to 8 was due to an enhanced electrostatic attraction between cationic species of MB with the negatively charged catalyst surface and resulting in enhanced sorption of the dye molecules on the catalyst surface. However, beyond pH 8, i.e. at pH 10.0, the percent removal was decreased. At higher Solution pH, the

MB molecules predominantly lies in the bulk solution where the concentration of hydroxyl radicals was insignificant²² hence, decreased its percent removal. Moreover, the concentration of hydroxyl radicals was decreased at high pH²⁵ which in turn decreased the photodegradation of MB. Similar findings were also reported in the degradation of methylene blue using TiO₂ nanocrystals supported on graphene-like bamboo charcoal.²⁶

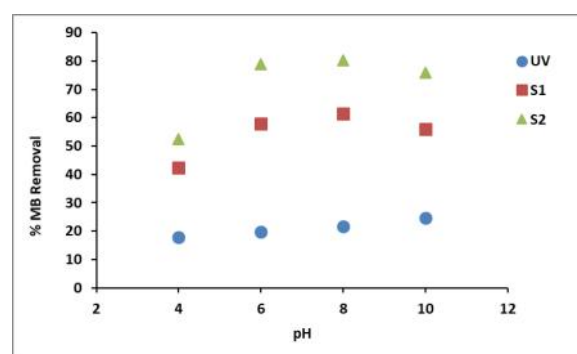


Figure 5 | Effect of pH in the photocatalytic degradation of methylene blue using UV, S1 and S2.

Effect of MB concentration

The effect of pollutant concentration was studied at varied MB concentrations, 1.0 to 10.0 mg/L at pH 6.0. The results obtained were represented as percent removal of MB as a function of initial MB concentration and returned in Fig. 6. The percent degradation of MB was increased from 66.67 to 86.66 % (by S2 sample); from 47.31 to 66.65 % (by S1 sample) and from 12.36 to 33.31% (by UV only) by decreasing the MB concentration from 10.0 to 1.0 mg/L, respectively. These results clearly indicated that the thin films S1 and S2 showed significantly higher photocatalytic activity compared to the UV only irradiated samples in the degradation of MB from aqueous solution. Furthermore, the PEG template thin film S2 sample had more enhanced photocatalytic activity than the S1 samples, since more MB molecules were effectively trapped inside the small mesopores provided by the catalyst surface, and hence, effectively oxidized by the

reactive species. The increased in MB concentration shielded the penetration of UV light into the pollutant solution, which introduced an inner filter effect and the solution became more impermeable for UV-radiations, which therefore limited the generation of active hydroxyl radicals and restricted the photocatalytic activity.²⁷

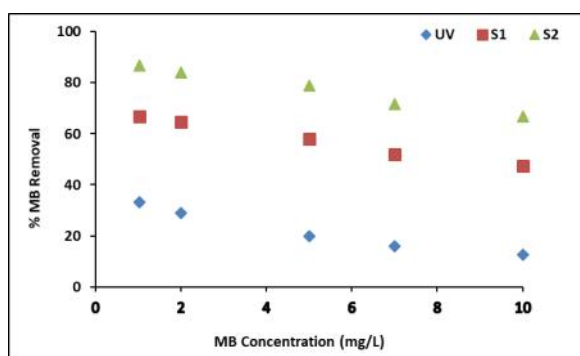


Figure 6 | Effect of concentration in the photocatalytic degradation of methylene blue using UV, S1 and S2.

Photocatalytic degradation kinetics of MB

The photo-catalytic degradation kinetics of MB was presented graphically in Fig. 7. The change in C_t/C_0 values were taken as a function of time 't' (where C_0 is the initial concentration of MB and C_t is the concentration of MB). A sharp decrease in degradation of MB was observed in presence of thin films S1 and S2 after the 2h UV irradiation. At the end of 2 h irradiation the C_t/C_0 values were found to be 0.21, 0.42 and 0.80 for the S2, S1 and photolysis only, respectively. A significant lower value of C_t/C_0 obtained using the S2 sample compared to the S1 sample confirmed the affinity of the pollutant towards the thin film (S2) surface with enhanced photo-catalytic degradation of MB at the surface. The kinetics of the MB degradation was represented using the known pseudo-first-order rate equation (Eq. 2):

$$r = -\frac{d[MB]}{dt} = k_{app} [k_{photolysis} + k_{photocatalysis}] = k_{app} [MB] \quad (2)$$

where, [MB] represents the concentration of dye pollutant and k_{app} is the pseudo-first-order rate constant. It is obvious that the k_{app} depends on the concentration of MB. Integration of Eq. (2) with the extreme conditions, i.e., at $t = 0$ the $[MB]=C_0$. Eq. (2) resulted in Eq. (3):

$$LN\left(\frac{C_0}{C_t}\right) = k_{app} \cdot t \quad (3)$$

Straight lines were drawn between the $LN(C_0/C_t)$ against time 't'. The results obtained were presented graphically in Fig. 7 (inset) for the MB photocatalytic degradation (initial concentration of MB: 5.0 mg/L and pH: 6.0). Moreover, the pseudo-first-order rate constants were evaluated at different concentrations using the UV, S1 and S2 samples and results were returned in Table 2. It was obvious that the apparent pseudo-first-order rate constant values were decreasing with increased in the concentration of MB. Therefore, the lower initial concentration of MB was found to be efficient in the photo-catalytic degradation using the thin films. On the other hand, UV only showed very slow and almost negligible degradation of MB compared with S1 and S2 samples.

Kinetics of photocatalytic oxidation of MB could be fitted with the Langmuir–Hinshelwood (L-H) equation which includes the adsorption properties of the adsorbate species on the photocatalyst surface. The derived equation (5) is used to its linear form:

$$r_0 = \frac{k_r \cdot K \cdot C_0}{1 + K \cdot C_0} \quad (4)$$

or

$$\frac{1}{r_0} = \frac{1}{K \cdot k_r} \cdot \frac{1}{C_0} + \frac{1}{k_r} \quad (5)$$

where '1/r₀' is the dependent variable, '1/C₀' the independent variable, 1/k_r is the linear coefficient and (1/(k_r·K)) the angular coefficient of the straight line. From this model, the L-H adsorption constant and the rate constant were obtained by plotting 1/r₀ against 1/C₀²⁸ also shown in Fig.8. The results

obtained for the k_r (mg/L/min) and K (L/mg) were found to be 0.115 and 0.089 (R^2 : 0.9997; for S1) and 0.090 and 0.201 (R^2 : 0.9995; for S2 sample), respectively. The L-H kinetic was reasonably fitted well to the photocatalytic degradation of MB using thin films.

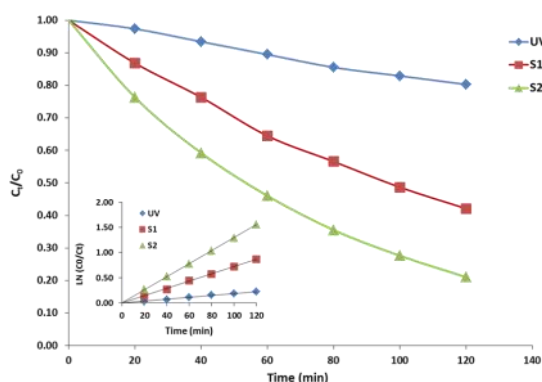


Figure 7 | Photocatalytic degradation of methylene blue as a function of time using thin films.

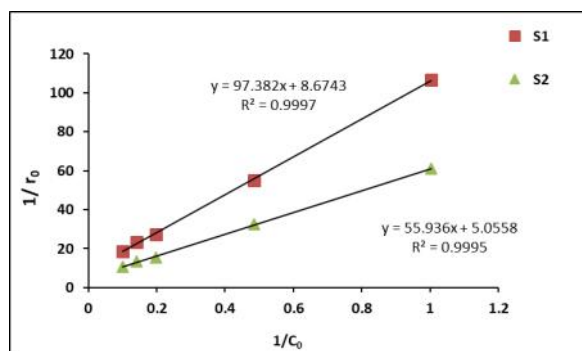


Figure 8 | Langmuir-Hinselwood Plot for the Photocatalytic degradation of methylene blue using thin films.

Effect of interfering ions

The applicability of thin film (S2) in the photocatalytic degradation of MB was assessed in presence of several interfering ions (5.0 mgL^{-1}): EDTA, sodium nitrite, sodium nitrate, sodium chloride, zinc chloride, copper sulfate, cadmium nitrate, gly-

cine and oxalic acid and. The sample solution with initial MB concentration of 1.0 mg/L was irradiated for 2 h at pH 6.0. The percent removal of MB was presented as a function of interfering ions and returned in Fig. 9. It was observed that the degradation of MB was hampered to a varied extent in the presence of different interfering ions. The inhibition caused by the co-existing ions in the reaction medium was mainly due to the scavenger properties of the cations or anions, as the photocatalytic degradation processes were predominantly driven by the highly oxidizing species, photogenerated valence band holes (h^+) or hydroxyl radicals ($\bullet\text{OH}$).

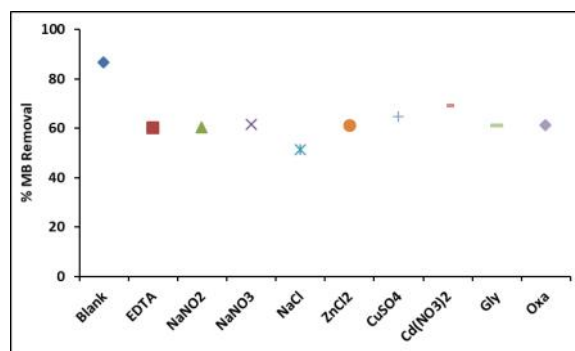


Figure 9 | Photocatalytic degradation of MB in presence of interfering ions using S2 thin film.

Mineralization of MB

The mineralization of MB was studied varying the pollutant concentration from 1.0 to 10.0 mg/L at constant pH 6.0 using S1 and S2 photocatalyst. Results were obtained at the end of 2 h of photoirradiation. Percent of TOC removal as a function of MB concentration was shown in Fig. 10. The results showed that increasing the concentration of MB from 1.0 to 10.0 mg/L the percent of TOC removal was decreased from 51.30 to 15.78 % (using S2 thin films) and 32.61 to 3.60% (using S1 thin films). However, prolonged irradiation, 24 h using S2 photocatalyst enabled to increase the TOC removal even up to 87.54 %. These results indicated that a partial mineralization of MB was achieved using the thin films; however, prolonged treatment may provide a

Table 2 | Kinetic data obtained in the photo-catalytic degradation of methylene blue using UV, S1 and S2.

Rate Constant ($k_{app} \times 10^{-3}$)					
(Initial concentration of MB in mg/L)					
	1	2	5	7	10
UV only	3.0 (0.949)	2.9 (0.889)	1.9 (0.989)	1.5 (0.945)	1.2 (0.998)
S1	9.4 (0.991)	8.8 (0.998)	7.2 (0.999)	6.1 (0.999)	4.8 (0.998)
S2	16.4 (0.995)	15.0 (0.996)	12.9 (0.999)	10.6 (0.998)	7.8 (0.997)

R^2 values are given in parenthesis.

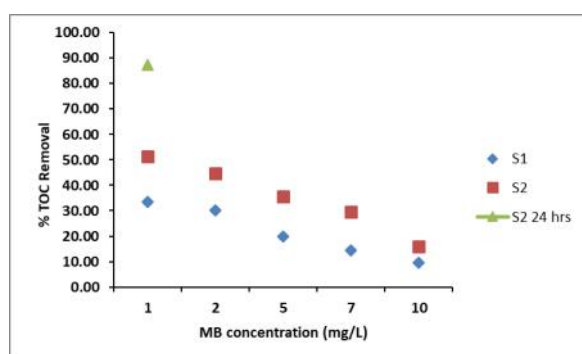


Figure 10 | Percent TOC removal as a function of MB concentration using thin films.

complete mineralization of MB from aqueous solutions. The low percent TOC removal rendered relatively a higher stability of the dye molecule with large aromatic ring structure as well as the intermediates formed after partial degradation in the photocatalytic reaction.

Conclusion

The Nanopillars-TiO₂ photocatalysts were obtained on the borosilicate glass substrate using the sol-gel template method with (S1) and without (S2) PEG (polyethylene glycol) as filler media. The thin films were well characterized with the XRD, SEM, AFM, FTIR and BET analytical methods. XRD data revealed that the S1 and S2 sample consist of anatase phase of TiO₂. SEM images showed fine grains of TiO₂ were evenly distributed on the substrate

and forming a uniform thin layer of TiO₂ particles for S1 sample. Whereas S2 sample possessed relatively disordered surface structure which has several micro-cracks on the surface. The IR data indicated the presence of -OH group with both the catalyst samples. AFM analytical data showed that the mean pillar size of TiO₂ particles was Ca 180 and 40 nm respectively for the S1 and S2 samples. Moreover, the average roughness (Ra) and root mean square roughness (Rq) were found to be 3.523, 14.06 nm and 2.708, 4.668 nm, respectively for S1 and S2 samples. Similarly, BET surface area for the S1 and S2 thin films were found to be 5.217 and 1.420 m²/g, with the pore size 7.77 and 4.16 nm, respectively.

These catalysts were further efficiently employed in the photocatalytic degradation of a methylene blue dye from aqueous solutions. Relatively, very high degradation occurred at pH 8.0, which was slightly decreased at higher pH conditions. Low MB initial concentration favored greatly the efficiency of photocatalyst in the percent degradation of MB. The degradation process was demonstrated with a pseudo-first-order rate kinetics and the data was fitted reasonably well with the Langmuir-Hinselwood rate Kinetics. The presence of several cations and anions hampered to some extent the photo-catalytic degradation of MB using the S2 photocatalyst. Overall the S1 and S2 thin films showed very high percent degradation of MB compared to the photolysis. S2 showed relatively higher photocatalytic efficiency compared to the S1

photocatalyst. Similarly, the mineralization of this dye increased with decreasing the pollutant concentration. The study conducted employing the thin films provide additional advantages with easy separation of catalyst as well as diminishing the shadowing effects commonly occurred with the TiO₂ powder or granules which enabled the S1 and S2 thin films to be potential and cost effective photocatalyst and could possess greater practical or industrial applicability.

References

1. Verma, A.K., Dash, R.R. & Bhunia, P. (2012). A review on chemical coagulation/flocculation technologies for removal of colour from textile wastewaters. *Journal of Environmental Management* **93**, 154–168.
2. Papic, S., Koprivanac, N., Bozic, A.L. & Metes, A. (2004). Removal of some reactive dyes from synthetic wastewater by combined Al (III) coagulation/carbon adsorption process. *Dyes and Pigments* **62**, 291–298.
3. Lee, Y.H., Matthews, R.D., Pavlostathis, S.G. (2006). Biological decolorization of reactive anthraquinone and phthalocyanine dyes under various oxidation-reduction conditions. *Water Environment Research* **78**, 156–169.
4. Riera-Torres, M., Gutierrez-Bouzan, C., & Crespi, M. (2010). Combination of coagulation–flocculation and nanofiltration techniques for dye removal and water reuse in textile effluents. *Desalination* **252**, 53–59.
5. Husain, Q. (2006). Potential applications of the oxidoreductive enzymes in the decolorization and detoxification of textile and other synthetic dyes from polluted water: a review. *Critical Reviews in Biotechnology* **26**, 201–221.
6. Hai, F.I., Yamamoto, K. & Fukushi, K. (2007). Hybrid treatment systems for dye wastewater. *Critical Reviews in Environmental Science and Technology* **37**, 315–377.
7. Gupta, V.K. & Suhas (2009). Application of low-cost adsorbents for dye removal: a review. *Journal of Environmental Management* **90**, 2313–2342.
8. Srinivasan, A. & Viraraghavan, T. (2010). Decolorization of dye wastewaters by biosorbents: A review. *Journal of Environmental Management* **91**, 1915–1929.
9. Ayodhya, G. & Veerabhadram, G. (2018). A review on recent advances in photodegradation of dyes using doped and heterojunction based semiconductor metal sulfide nanostructures for environmental protection. *Materials Today Energy* **9**, 83–113.
10. Adeleke, J.T., Theivasanthi, T., Thiruppathi, M., Swaminathan, M., Akomolafe, T. & Alabi, A.B. (2018). Photocatalytic degradation of methylene blue by ZnO/NiFe₂O₄ nanoparticles. *Applied Surface Science*, **455**, 195–200.
11. Zangeneh, H., Zinatizadeh, A.A.L., Habibi, M., Akia, M. & Hasnain Isa, M. (2015). Photocatalytic oxidation of organic dyes and pollutants in wastewater using different modified titanium dioxides: A comparative review. *Journal of Industrial and Engineering Chemistry* **26**, 1–36.
12. Ariyanti, D., Maillot, M. & Gao, W. (2018). Photo-assisted degradation of dyes in a binary system using TiO₂ under simulated solar radiation. *Journal of Environmental Chemical Engineering* **6**, 539–548.
13. Nguyen, C.H., Fu, C.C. & Juang, R.S. (2018). Degradation of methylene blue and methyl orange by palladium-doped TiO₂ photocatalysis for water reuse: Efficiency and degradation pathways 2018. *Journal of Cleaner Production*. doi.10.1016/j.jclepro.2018.08.110.
14. Shah, J., Jan, M.R. & Khitab, F. (2018). Sonophotocatalytic degradation of textile dyes over Cu impregnated ZnO catalyst in aqueous solution. *Process Safety and Environmental Protection* **16**, 149–158.
15. Ayodhya, D. & Veerabhadram, G. (2018). A review on recent advances in photodegradation of dyes using doped and heterojunction based semiconductor metal sulfide nanostructures for environmental protection. *Materials Today Energy* **9**, 83–113.
16. Fujishima, A., Zhang X. & Tryk, D.A. (2008). TiO₂ photocatalysis and related surface phenomena. *Surface Science Report* **63**, 515–582.
17. Arbuj, S.S., Hawaldar, R.R., Mulik, U.P., Wani, B.N., Amalnerkar, D.P. & Waghmode, S.B. (2010). Preparation, characterization and photocatalytic activity of TiO₂ towards methylene blue degradation. *Materials Science and Engineering B* **168**, 90–94.
18. Lachheb, H., Puzenat, E., Houas, A., Ksibi, M., Elaloui, E., Guillard, C. & Herrmann, J.M. (2002). Photocatalytic degradation of various types of dyes (Alizarin S, Crocein Orange G, Methyl Red, Congo Red, Methylene Blue) in water by UV-irradiated titania. *Applied Cataly-*

- sis B: *Environmental* **39**, 75–90.
19. Yu, W., Liu, X., Pan, L., Li, J., Liu, J., Zhang, J., Li, P., Chen, C. & Sun, Z. (2014). Enhanced visible light photocatalytic degradation of methylene blue by F-doped TiO₂. *Applied Surface Science* **319**, 107–112.
 20. Tiwari, A., Shukla, A., Lalliansanga., Tiwari, D. & Lee, S.M. (2018). Nanocomposite thin films Ag⁰(NP)/TiO₂ in the efficient removal of micro-pollutants from aqueous solutions: A case study of tetracycline and sulfamethoxazole removal. *Journal of Environmental Management* **220** (15), 96–108.
 21. Singh, J., Khan, S.A., Shah, J., Kotnala, R.K. & Mohapatra, S. (2017). Nanostructured TiO₂ thin films prepared by RF magnetron sputtering for photocatalytic applications. *Applied Surface Science* **422**, 953–961.
 22. Lalhriatpuia, C., Tiwari, D., Tiwari, A. & Lee, S.M. (2015). Immobilized Nanopillars-TiO₂ in the efficient removal of micro-pollutants from aqueous solutions: Physico-chemical studies. *Chemical Engineering Journal* **281**, 782–792.
 23. Tiwari, D., Lalhriatpuia, C., Lalmunsiam., Lee, S.M. & Kong, S.H. (2015). Efficient application of nano-TiO₂ thin films in the photocatalytic removal of Alizarin Yellow from aqueous solutions. *Applied Surface Science* **353**, 275–283.
 24. Lalhriatpuia, C. & Tiwari, D. (2015). Immobilised nanopillars TiO₂ in the photocatalytic degradation of methyl thymol blue from aqueous solutions: Batch reactor studies. *Science and Technology Journal* **3**(2), 38–49.
 25. Wang, Y.B. & Hong, C.S. (1999). Effect of hydrogen peroxide, periodate and persulfate on photocatalysis of 2-chlorobiphenyl in aqueous TiO₂ suspensions. *Water Research* **33** (9), 2031–2036.
 26. Wu, F., Liu, W., Qiu, J., Li, J., Zhou, W., Fang, Y., Zhang, S. & Li, X. (2015). Enhanced photocatalytic degradation and adsorption of methylene blue via TiO₂nanocrystals supported on graphene-like bamboo charcoal. *Applied Surface Science* **358** (A), 425–435.
 27. Ejhieh, N. & Mobarakeh, Z. (2014). Heterogeneous photodecolorization of mixture of methylene blue and bromophenol blue using CuO-nano-clinoptilolite. *Journal of Industrial and Engineering Chemistry* **20**, 1421–1431.
 28. Wang, K.H., Hisieh, Y.H., Wu, C.H. & Chang, C.Y. (2000). The pH and anion effects on the heterogeneous photocatalytic degradation of o-methylbenzoic acid in TiO₂ aqueous suspension. *Chemosphere* **40**, 389–394.